SCIENTIFIC REPORTS

OPEN

Deep sequencing of primary human lung epithelial cells challenged with H5N1 influenza virus reveals a proviral role for CEACAM1

Received: 9 July 2018
Accepted: 25 September 2018
Published online: 19 October 2018

Siying Ye[1,2], Christopher J. Cowled[3], Cheng-Hon Yap[4] & John Stambas[1,2]

Current prophylactic and therapeutic strategies targeting human influenza viruses include vaccines and antivirals. Given variable rates of vaccine efficacy and antiviral resistance, alternative strategies are urgently required to improve disease outcomes. Here we describe the use of HiSeq deep sequencing to analyze host gene expression in primary human alveolar epithelial type II cells infected with highly pathogenic avian influenza H5N1 virus. At 24 hours post-infection, 623 host genes were significantly upregulated, including the cell adhesion molecule *CEACAM1*. H5N1 virus infection stimulated significantly higher CEACAM1 protein expression when compared to influenza A PR8 (H1N1) virus, suggesting a key role for CEACAM1 in influenza virus pathogenicity. Furthermore, silencing of endogenous *CEACAM1* resulted in reduced levels of proinflammatory cytokine/chemokine production, as well as reduced levels of virus replication following H5N1 infection. Our study provides evidence for the involvement of CEACAM1 in a clinically relevant model of H5N1 infection and may assist in the development of host-oriented antiviral strategies.

Influenza viruses cause acute and highly contagious seasonal respiratory disease in all age groups. Between 3–5 million cases of severe influenza-related illness and over 250 000 deaths are reported every year. In addition to constant seasonal outbreaks, highly pathogenic avian influenza (HPAI) strains, such as H5N1, remain an ongoing pandemic threat with recent WHO figures showing 454 confirmed laboratory infections and a mortality rate of 53%. It is important to note that humans have very little pre-existing immunity towards avian influenza virus strains. Moreover, there is no commercially available human H5N1 vaccine. Given the potential for H5N1 viruses to trigger a pandemic[1,2], there is an urgent need to develop novel therapeutic interventions to combat known deficiencies in our ability to control outbreaks. Current seasonal influenza virus prophylactic and therapeutic strategies involve the use of vaccination and antivirals. Vaccine efficacy is highly variable as evidenced by a particularly severe 2017/18 epidemic, and frequent re-formulation of the vaccine is required to combat ongoing mutations in the influenza virus genome. In addition, antiviral resistance has been reported for many circulating strains, including the avian influenza H7N9 virus that emerged in 2013[3,4]. Influenza A viruses have also been shown to target and hijack multiple host cellular pathways to promote survival and replication[5,6]. As such, there is increasing evidence to suggest that targeting host pathways will influence virus replication, inflammation, immunity and pathology[5,7]. Alternative intervention strategies based on modulation of the host response could be used to supplement the current prophylactic and therapeutic protocols.

While the impact of influenza virus infection has been relatively well studied in animal models[8,9], human cellular responses are poorly defined due to the lack of available human autopsy material, especially from HPAI virus-infected patients. In the present study, we characterized influenza virus infection of primary human alveolar epithelial type II (ATII) cells isolated from normal human lung tissue donated by patients undergoing lung resection. ATII cells are a physiologically relevant infection model as they are a main target for influenza A viruses when entering the respiratory tract[10]. Human host gene expression following HPAI H5N1 virus (A/Chicken/Vietnam/0008/04) infection of primary ATII cells was analyzed using Illumina HiSeq deep sequencing. In order to

[1]School of Medicine, Deakin University, Waurn Ponds, Victoria, Australia. [2]AAHL CSIRO Deakin Collaborative Biosecurity Laboratory, East Geelong, Victoria, Australia. [3]Health & Biosecurity, CSIRO, East Geelong, Victoria, Australia. [4]University Hospital Geelong, Barwon Health, Geelong, Victoria, Australia. Correspondence and requests for materials should be addressed to S.Y. (email: siying.ye@csiro.au)

gain a better understanding of the mechanisms underlying modulation of host immunity in an anti-inflammatory environment, we also analyzed changes in gene expression following HPAI H5N1 infection in the presence of the reactive oxygen species (ROS) inhibitor, apocynin, a compound known to interfere with NADPH oxidase subunit assembly[5,6].

The HiSeq analysis described herein has focused on differentially regulated genes following H5N1 infection. Several criteria were considered when choosing a "hit" for further study. These included: (1) Novelty; has this gene been studied before in the context of influenza virus infection/pathogenesis? (2) Immunoregulation; does this gene have a regulatory role in host immune responses so that it has the potential to be manipulated to improve immunity? (3) Therapeutic reagents; are there any existing commercially available therapeutic reagents, such as specific inhibitors or inhibitory antibodies that can be utilized for *in vitro* and *in vivo* study in order to optimize therapeutic strategies? (4) Animal models; is there a knock-out mouse model available for *in vivo* influenza infection studies? Based on these criteria, carcinoembryonic-antigen (CEA)-related cell adhesion molecule 1 (*CEACAM1*) was chosen as a key gene of interest. CEACAM1 (also known as BGP or CD66) is expressed on epithelial and endothelial cells[11], as well as B cells, T cells, neutrophils, NK cells, macrophages and dendritic cells (DCs)[12–14]. Human CEACAM1 has been shown to act as a receptor for several human bacterial and fungal pathogens, including *Haemophilus influenza*, *Escherichia coli*, *Salmonella typhi and Candida albicans*, but has not as yet been implicated in virus entry[15–17]. There is however emerging evidence to suggest that CEACAM1 is involved in host immunity as enhanced expression in lymphocytes was detected in pregnant women infected with cytomegalovirus[18] and in cervical tissue isolated from patients with papillomavirus infection[19].

Eleven *CEACAM1* splice variants have been reported in humans[20]. CEACAM1 isoforms (Uniprot P13688-1 to -11) can differ in the number of immunoglobulin-like domains present, in the presence or absence of a transmembrane domain and/or the length of their cytoplasmic tail (i.e. L, long or S, short). The full-length human CEACAM1 protein (CEACAM1-4L) consists of four extracellular domains (one extracellular immunoglobulin variable-region-like (IgV-like) domain and three immunoglobulin constant region 2-like (IgC2-like) domains), a transmembrane domain, and a long (L) cytoplasmic tail. The long cytoplasmic tail contains two immunoreceptor tyrosine-based inhibitory motifs (ITIMs) that are absent in the short form[20]. The most common isoforms expressed by human immune cells are CEACAM1-4L and CEACAM1-3L[21]. CEACAM1 interacts homophilically with itself[22] or heterophilically with CEACAM5 (a related CEACAM family member)[23]. The dimeric state allows recruitment of signaling molecules such as SRC-family kinases, including the tyrosine phosphatase SRC homology 2 (SH2)-domain containing protein tyrosine phosphatase 1 (SHP1) and SHP2 members to phosphorylate ITIMs[24]. As such, the presence or absence of ITIMs in CEACAM1 isoforms influences signaling properties and downstream cellular function. CEACAM1 homophilic or heterophilic interactions and ITIM phosphorylation are critical for many biological processes, including regulation of lymphocyte function, immunosurveillance, cell growth and differentiation[25,26] and neutrophil activation and adhesion to target cells during inflammatory responses[27]. It should be noted that CEACAM1 expression has been modulated *in vivo* using an anti-CEACAM1 antibody (MRG1) to inhibit CEACAM1-positive melanoma xenograft growth in SCID/NOD mice[28]. MRG1 blocked CEACAM1 homophilic interactions that inhibit T cell effector function, enhancing the killing of CEACAM1+ melanoma cells by T cells[28]. This highlights a potential intervention pathway that can be exploited in other disease processes, including virus infection. In addition, *Ceacam1*-knockout mice are available for further *in vivo* infection studies.

Our results show that CEACAM1 mRNA and protein expression levels were highly elevated following HPAI H5N1 infection. Furthermore, small interfering RNA (siRNA)-mediated inhibition of CEACAM1 reduced inflammatory cytokine and chemokine production, and more importantly, inhibited H5N1 virus replication in primary human ATII cells and in the continuous human type II respiratory epithelial A549 cell line. Taken together, these observations suggest that CEACAM1 is an attractive candidate for modulating influenza-specific immunity. In summary, our study has identified a novel target that may influence HPAI H5N1 immunity and serves to highlight the importance of manipulating host responses as a way of improving disease outcomes in the context of virus infection.

Results

Three experimental groups were included in the HiSeq analysis of H5N1 infection in the presence or absence of the ROS inhibitor, apocynin: (i) uninfected cells treated with 1% DMSO (vehicle control) (ND), (ii) H5N1-infected cells treated with 1% DMSO (HD) and (iii) H5N1-infected cells treated with 1 mM apocynin dissolved in DMSO (HA). These three groups were assessed using pairwise comparisons: ND *vs*. HD, ND *vs*. HA, and HD *vs*. HA.

H5N1 infection and apocynin treatment induce differential expression of host genes. ATII cells isolated from human patients[29,30] were infected with H5N1 on the apical side at a multiplicity of infection (MOI) of 2 for 24 hours and RNA extracted. HiSeq was performed on samples and reads mapped to the human genome where they were then assembled into transcriptomes for differential expression analysis. A total of 13,649 genes were identified with FPKM (fragments per kilobase of exon per million fragments mapped) > 1 in at least one of the three experimental groups. A total of 623 genes were significantly upregulated and 239 genes were significantly downregulated (q value < 0.05, $\geq$2-fold change) following H5N1 infection (ND *vs*. HD) (Fig. 1A; Table S1). HPAI H5N1 infection of ATII cells activated an antiviral state as evidenced by the upregulation of numerous interferon-induced genes, genes associated with pathogen defense, cell proliferation, apoptosis, and metabolism (Table 1; Table S2). In addition, Kyoto Encyclopedia of Genes and Genomes (KEGG) pathway mapping showed that many of the upregulated genes in the HD group were mapped to TNF signaling (hsa04668), Toll-like receptor signaling (hsa04620), cytokine-cytokine receptor interaction (hsa04060) and RIG-I-like receptor signaling (hsa04622) (Table 2, Table S3).

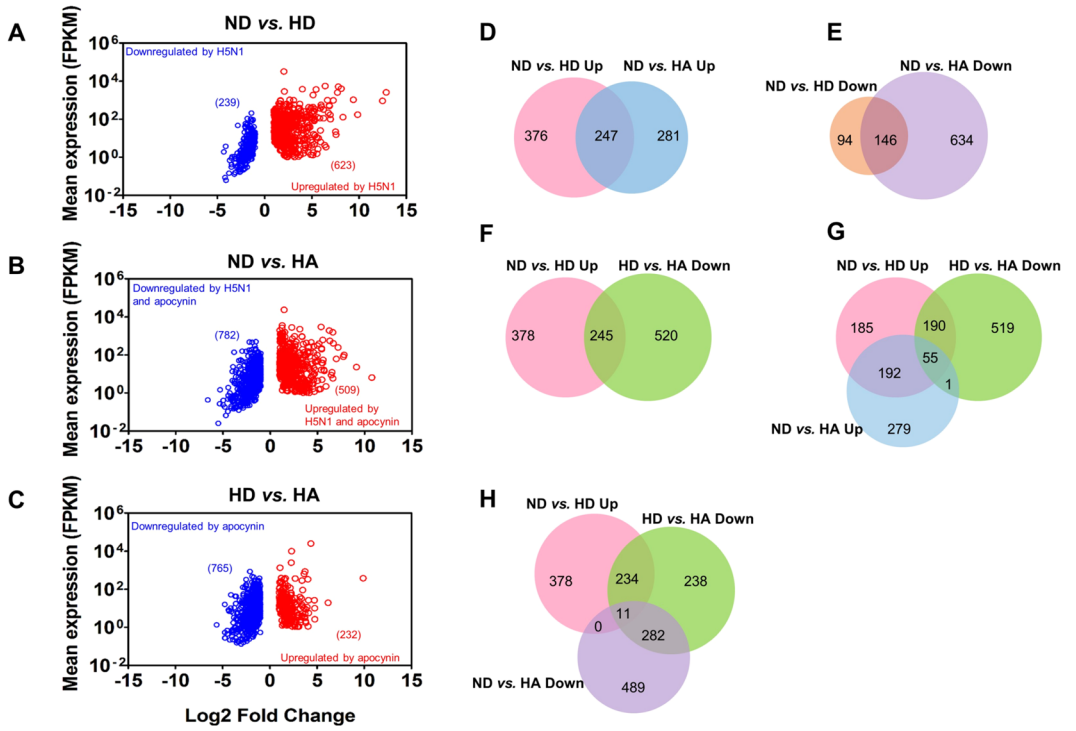

Figure 1. Human host gene expression profiles following HPAI H5N1 infection and apocynin treatment. Genes that were statistically upregulated (shown as red circles) or downregulated (shown as blue circles) were assessed in pairwise comparisons as indicated. Data are plotted as the mean FPKM of each gene obtained from HD or HA against a Log2 fold change compared to ND as (**A**) ND *vs.* HD or (**B**) ND *vs.* HA, or compared to HD as (**C**) HD *vs.* HA. (**D–H**) The number and overlap of genes in each pairwise comparison is illustrated by Venn diagrams. ND, uninfected cells treated with 1% DMSO vehicle control; HD and HA, cells infected with H5N1 at a MOI of 2 for 24 hours in the presence of 1% DMSO or 1 mM apocynin, respectively. Up; upregulated. Down; downregulated. FPKM; fragments per kilobase of exon per million fragments mapped. RNA samples were obtained from ATII cells isolated from the lung tissue of three donors. The full list of transcripts identified in the HiSeq analysis, as well as differentially regulated transcripts in the three experimental groups is presented in Table S1.

In the H5N1-infected and apocynin-treated (HA) group, a large number of genes were also significantly upregulated (509 genes) or downregulated (782 genes) (Fig. 1B; Table S1) relative to the ND control group. Whilst a subset of genes was differentially expressed in both the HD and HA groups, either being upregulated (247 genes, Fig. 1D) or downregulated (146 genes, Fig. 1E), a majority of genes did not in fact overlap between the HD and HA groups (Fig. 1D, E). This suggests that apocynin treatment can affect gene expression independent of H5N1 infection. Gene Ontology (GO) enrichment analysis of genes upregulated by apocynin showed the involvement of the type I interferon signaling pathway (GO:0060337), the defense response to virus (GO:0009615), negative regulation of viral processes (GO:48525) and the response to stress (GO:0006950) (Table S2, "ND *vs.* HA Up"). Genes downregulated by apocynin include those that are involved in cell adhesion (GO:0007155), regulation of cell migration (GO:0030334), regulation of cell proliferation (GO:0042127), signal transduction (GO:0007165) and oxidation-reduction processes (GO:0055114) (Table S2, "ND *vs.* HA Down").

A total of 623 genes were upregulated following H5N1 infection ("ND *vs.* HD Up", Fig. 1F). By overlapping the two lists of genes from "ND *vs.* HD Up" and "HD *vs.* HA Down", 245 genes were shown to be downregulated in the presence of apocynin (Fig. 1F). By overlapping three lists of genes from "ND *vs.* HD Up", "HD *vs.* HA Down" and "ND *vs.* HA Up", 55 genes out of the 245 genes (190 plus 55 genes) were present in all three lists (Fig. 1G), indicating that these 55 genes were significantly inhibited by apocynin but to a level that was still significantly higher than that in uninfected cells. The 55 genes include those involved in influenza A immunity (hsa05164; DDX58, IFIH1, IFNB1, MYD88, PML, STAT2), Jak-STAT signaling (hsa04630; IFNB1, IL15RA, IL22RA1, STAT2), RIG-I-like receptor signaling (hsa04622; DDX58, IFIH1, IFNB1) and Antigen processing and presentation (hsa04612; TAP2, TAP1, HLA-DOB) (Tables S3 and S4). Therefore, critical immune responses induced following H5N1 infection were not dampened following apocynin treatment. The remaining 190 of 245 genes were not present in the "ND *vs.* HA Up" list, suggesting that those genes were significantly inhibited by apocynin to a level that was similar to uninfected control cells (Fig. 1G). The 190 genes include those involved in TNF signaling (hsa04668; CASP10, CCL2, CCL5, CFLAR, CXCL5, END1, IL6, TRAF1, VEGFC), cytokine-cytokine receptor interaction (hsa04060; VEGFC, IL6, CCL2, CXCL5, CXCL16, IL2RG, CD40, CCL5, CCL7, IL1A), NF-kappa B signaling pathway (hsa04064: TRAF1, CFLAR, CARD11, TNFSF13B, TICAM1, CD40) and PI3K-Akt signaling (hsa04151; CCND1, GNB4, IL2RG, IL6, ITGA2, JAK2, LAMA1, MYC, IPK3AP1, TLR2, VEGFC) (Tables S3 and S4). This is consistent with the role of apocynin in reducing inflammation[31].

GO Terms (Biological Processes)	Gene Count	FDR q value
GO:0006952 defense response	99	5.00E-29
GO:0043207 response to external biotic stimulus	87	1.34E-27
GO:0009615 response to virus	49	3.02E-22
GO:0002376 immune system process	145	6.32E-24
GO:0006955 immune response	76	4.71E-20
GO:0019221 cytokine-mediated signaling pathway	67	7.74E-19
GO:0060337 type I interferon signaling pathway	22	1.37E-17
GO:0006950 response to stress	177	1.45E-17
GO:0007166 cell surface receptor signaling pathway	137	3.01E-17
GO:0001817 regulation of cytokine production	65	5.99E-16
GO:0045088 regulation of innate immune response	51	1.90E-15
GO:0060333 interferon-gamma-mediated signaling pathway	20	3.57E-13
GO:0006954 inflammatory response	41	1.36E-11
GO:1903900 regulation of viral life cycle	25	4.83E-09
GO:0042127 regulation of cell proliferation	94	5.01E-09

Table 1. GO terms enriched in significantly upregulated genes in response to H5N1 infection ("ND *vs.* HD") in ATII cells. The full list of GO term enrichment is presented in Table S2.

KEGG Pathways	Number of Genes	P-value	Fold Enrichment
hsa05168: Herpes simplex infection	37	3.49E-15	4.75
hsa05164: Influenza A	29	7.04E-10	3.92
hsa05162: Measles	24	6.08E-09	4.24
hsa04668: TNF signaling pathway	20	7.34E-08	4.43
hsa04620: Toll-like receptor signaling pathway	19	3.82E-07	4.21
hsa05203: Viral carcinogenesis	27	4.34E-07	3.10
hsa05160: Hepatitis C	20	2.79E-06	3.53
hsa05161: Hepatitis B	20	1.02E-05	3.24
hsa04060: Cytokine-cytokine receptor interaction	25	3.64E-05	2.55
hsa04630: Jak-STAT signaling pathway	19	3.68E-05	3.08
hsa05332: Graft-versus-host disease	9	5.22E-05	6.41
hsa04623: Cytosolic DNA-sensing pathway	12	6.58E-05	4.41
hsa04622: RIG-I-like receptor signaling pathway	12	1.53E-04	4.03
hsa04064: NF-kappa B signaling pathway	13	2.76E-04	3.51
hsa04514: Cell adhesion molecules (CAMs)	17	3.12E-04	2.81

Table 2. Representatives of over-represented KEGG pathways with a maximum P-value of 0.05 and the number of genes contributing to each pathway that is significantly upregulated following H5N1 infection ("ND *vs.* HD Up"). The full list of KEGG pathways is presented in Table S3.

By overlapping the three lists of genes from "ND *vs.* HD Up", "HD *vs.* HA Down" and "ND *vs.* HA Down", 11 genes were found in all three comparisons (Fig. 1H). This suggests that these 11 genes are upregulated following H5N1 infection and are significantly reduced by apocynin treatment to a level lower than that observed in uninfected control cells (Fig. 1H). Among these were inflammatory cytokines/chemokines genes, including CXCL5, IL1A, AXL (a member of the TAM receptor family of receptor tyrosine kinases) and TMEM173/STING (Stimulator of IFN Genes) (Table S4).

Our previous study demonstrated that H5N1 infection of A549 cells in the presence of apocynin enhanced expression of negative regulators of cytokine signaling (SOCS), SOCS1 and SOCS3[6]. This, in turn, resulted in a reduction of H5N1-stimulated cytokine and chemokine production (*IL6*, *IFNB1*, *CXCL10* and *CCL5* in A549 cells), which was not attributed to lower virus replication as virus titers were not affected by apocynin treatment[6]. We performed a qRT-PCR analysis on the same RNA samples submitted for HiSeq analysis to validate HiSeq results. *IL6* (Fig. 2A), *IFNB1* (Fig. 2B), *CXCL10* (Fig. 2C), and *CCL5* (Fig. 2D) gene expression was significantly elevated in ATII cells following infection and was reduced by the addition of apocynin (except for *IFNB1*). Consistent with previous findings in A549 cells[6], H5N1 infection alone induced the expression of *SOCS1* as shown by HiSeq and qRT-PCR analysis (Fig. 2E). Apocynin treatment further increased *SOCS1* mRNA expression (Fig. 2E). Although HiSeq analysis did not detect a statistically significant increase of *SOCS1* following apocynin treatment, the Log2 fold-changes in *SOCS1* gene expression were similar between the HD and HA groups (4.8-fold *vs* 4.0-fold) (Fig. 2E). HiSeq analysis of *SOCS3* transcription showed significant increase following H5N1 infection and apocynin treatment (Fig. 2F). qRT-PCR analysis showed that although *SOCS3* mRNA was only slightly increased following H5N1 infection, it was further significantly upregulated in the presence

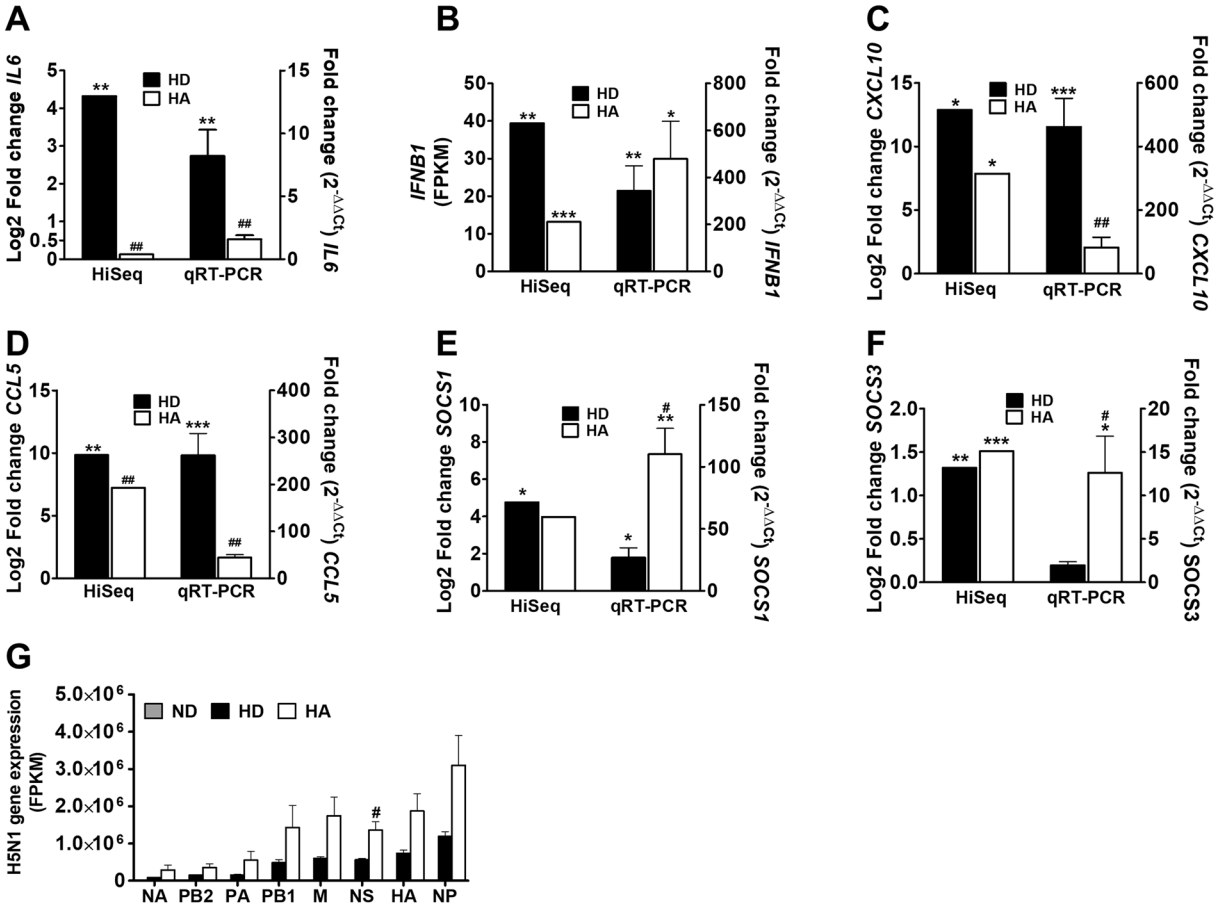

Figure 2. Hiseq analysis of H5N1 influenza virus gene expression and validation of differential gene expression identified with HiSeq using qRT-PCR. The same RNA samples used for HiSeq analysis were also subjected to qRT-PCR analysis of (**A**) *IL6*, (**B**) *IFNB1*, (**C**) *CXCL10*, (**D**) *CCL5*, (**E**) *SOCS1* and (**F**) *SOCS3* mRNA expression in three experimental groups of ATII cells (ND, HD and HA). Fold-changes following qRT-PCR analysis were calculated using $2^{-\Delta\Delta Ct}$ method (right Y axis) normalized to β-*actin* and compared with the ND group. Data from HiSeq was calculated as Log2 fold-change (left Y axis) compared with the ND group. *IFNB1* transcription was not detected in ND, therefore HiSeq *IFNB1* data from HD and HA groups was expressed as FPKM. $^{*}p < 0.05$ and $^{**}p < 0.01$, $^{***}p < 0.001$ compared with ND; $^{\#}p < 0.05$, $^{\#\#}p < 0.01$, compared with HD. (**G**) Hiseq analysis of H5N1 influenza virus gene expression profiles with or without apocynin treatment in primary human ATII cells. $^{\#}p < 0.05$, compared with HD.

of apocynin (Fig. 2F). Therefore, apocynin also contributes to the reduction of H5N1-stimulated cytokine and chemokine production in ATII cells.

Apocynin, a compound that inhibits production of ROS, has been shown to influence influenza-specific responses *in vitro*[6] and *in vivo*[5]. Although virus titers are not affected by apocynin treatment *in vitro*[6], some anti-viral activity is observed *in vivo* when mice have been infected with a low pathogenic A/HongKong/X31 H3N2 virus[6]. HiSeq analysis of HPAI H5N1 virus gene transcription showed that although there was a trend for increased influenza virus gene expression following apocynin treatment, only influenza non-structural (NS) gene expression was significantly increased (Fig. 2G). The reduced cytokine and chemokine production in H5N1-infected ATII cells (Fig. 2A–F) is unlikely to be associated with lower virus replication.

Enrichment of antiviral and immune response genes in HPAI H5N1-infected ATII cells. GO enrichment analysis was performed on genes that were significantly upregulated following HPAI H5N1 infection in ATII cells in the presence or absence of apocynin to identify over-presented GO terms. Many of the H5N1-upregulated genes were broadly involved in defense response (GO:0006952), response to external biotic stimulus (GO:0043207), immune system processes (GO:0002376), cytokine-mediated signaling pathway (GO:0019221) and type I interferon signaling pathway (GO:0060337) (Table 1; Table S2). In addition, many of the H5N1-upregulated genes mapped to metabolic pathways (hsa01100), cytokine-cytokine receptor interaction (hsa04060), Influenza A (hsa05164), TNF signaling (hsa04668) or Jak-STAT signaling (hsa04630) (Table S3). However, not all the H5N1-upregulated genes in these pathways were inhibited by apocynin treatment as mentioned above (Fig. 1F; Table S3).

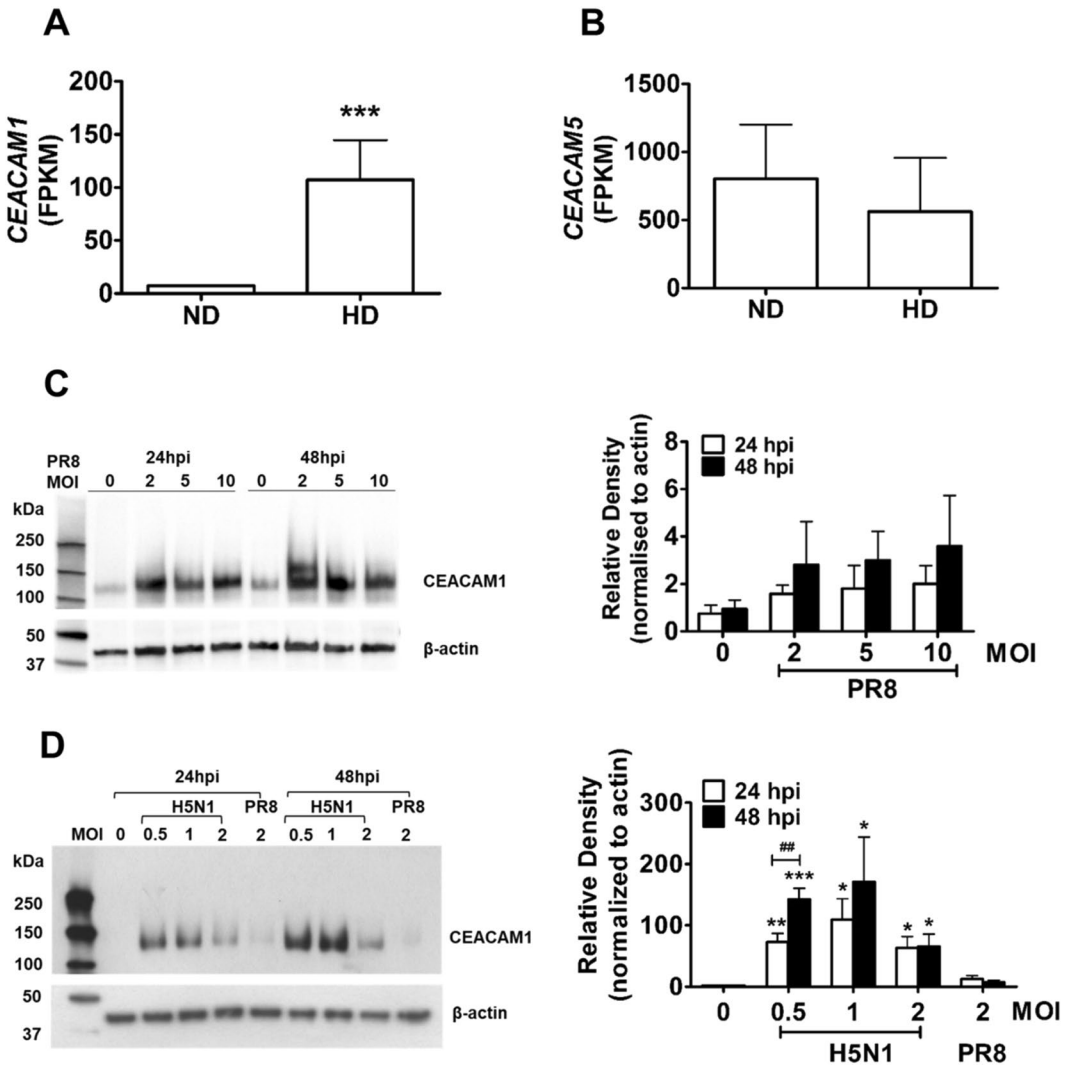

Figure 3. Upregulation of CEACAM1 in influenza virus-infected cells. (**A**) HiSeq analysis showed elevated transcription of *CEACAM1* in H5N1-infected ATII cells (HD) when compared to uninfected cells (ND). $***p < 0.01$, compared with ND. (**B**) The transcription level of a related CEACAM family member, *CEACAM5*, was not altered following H5N1 infection. (**C**) A representative Western blot of three individual experiments and protein band density analysis of endogenous CEACAM1 protein expression in A549 cells following infection with PR8 virus at MOIs of 2, 5 and 10 at 24 and 48 hpi. (**D**) A representative Western blot of three individual experiments and protein band density analysis of endogenous CEACAM1 protein expression in primary human ATII cells infected with PR8 or HPAI H5N1 virus at various MOIs and time points as indicated. $*p < 0.05$, $**p < 0.01$, $***p < 0.001$, compared with PR8 at the corresponding time point. $^{\#\#}p < 0.01$, compared between 24 and 48 hpi. All samples on protein blots were run and cropped from the same gel for accurate standardization. Full blots are provided in the supplementary data file.

Upregulation of the cell adhesion molecule CEACAM1 in H5N1-infected ATII cells. The cell adhesion molecule CEACAM1 has been shown to be critical for the regulation of immune responses during infection, inflammation and cancer[20]. The *CEACAM1* transcript was significantly upregulated following H5N1 infection (Fig. 3A). In contrast, a related member of the CEACAM family, *CEACAM5*, was not affected by H5N1 infection (Fig. 3B). It is also worth noting that more reads were obtained for *CEACAM5* (>1000 FPKM) (Fig. 3B) than *CEACAM1* (~7 FPKM) (Fig. 3A) in uninfected ATII cells, which is consistent with their normal expression patterns in human lung tissue[32]. Therefore, although CEACAM1 forms heterodimers with CEACAM5[23], the higher basal expression of *CEACAM5* in ATII cells may explain why its expression was not enhanced by H5N1 infection. Endogenous CEACAM1 protein expression was also analyzed in uninfected or influenza virus-infected A549 (Fig. 3C) and ATII cells (Fig. 3D). CEACAM1 protein expression was slightly, but not significantly, increased in A549 cells infected with A/Puerto Rico/8/1934 H1N1 (PR8) virus for 24 or 48 hours when compared to uninfected cells (Fig. 3C). No significant difference in CEACAM1 protein levels were observed at various MOIs (2, 5 or 10) or between the 24 and 48 hpi timepoints (Fig. 3C).

After examing CEACAM1 protein expression following infection with PR8 virus in A549 cells, CEACAM1 protein expression was then examined in primary human ATII cells infected with HPAI H5N1 and compared

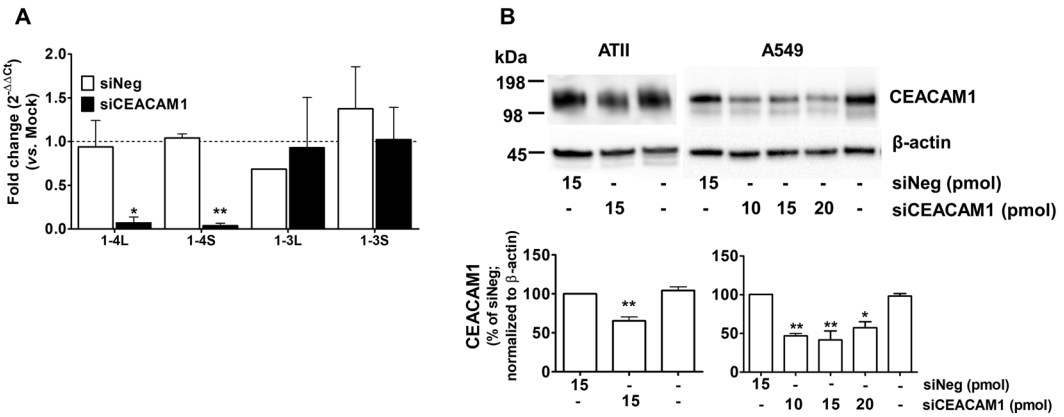

Figure 4. siRNA-mediated silencing of *CEACAM1* in ATII and A549 cells. (**A**) SYBR Green qRT-PCR analysis of siRNA-mediated silencing of endogenous *CEACAM1-4L*, *-4S*, *-3L and -3S* in ATII cells compared to cells transfected with siNeg controls. Data are expressed as fold-change ($2^{-\Delta\Delta Ct}$ method) normalized to *β-actin* and compared to mock-transfected cells that have a fold-change of 1 (dotted line). $*p < 0.05$, $**p < 0.01$. qRT-PCR was performed in duplicate and ATII cells were cultured from three donors. (**B**) A representative Western blot of three individual experiments and protein band density analysis of siCEACAM1-mediated knockdown of endogenous CEACAM1 in ATII and A549 cells transfected with siCEACAM1 or siNeg control or in mock-transfected cells. $*p < 0.05$, $**p < 0.01$, compared to siNeg control. Experiments were performed using ATII cells from three donors and three different passages of A549 cells. All samples on protein blots were run and cropped from the same gel for accurate standardization. Full blots are provided in the supplementary data file.

to PR8 virus infection (Fig. 3D). ATII cells were infected with PR8 virus at a MOI of 2, a dose that induced upregulation of cytokines and influenza Matrix (M) gene analyzed by qRT-PCR (data not shown). Lower MOIs of 0.5, 1 and 2 of HPAI H5N1 were tested due to the strong cytopathogenic effect H5N1 causes at higher MOIs. Endogenous CEACAM1 protein levels were significantly and similarly elevated in H5N1-infected ATII cells at the three MOIs tested. CEACAM1 protein expression in ATII cells infected with H5N1 at MOIs of 0.5 were higher at 48 hpi than those observed at 24 hpi (Fig. 3D). HPAI H5N1 virus infection at MOIs of 0.5, 1 and 2 stimulated higher endogenous levels of CEACAM1 protein expression when compared to PR8 virus infection at a MOI of 2 at the corresponding time point (a maximum ~9-fold increase induced by H5N1 at MOIs of 0.5 and 1 at 48 hpi when compared to PR8 at MOI of 2), suggesting a possible role for CEACAM1 in influenza virus pathogenicity (Fig. 3D).

Knockdown of endogenous CEACAM1 inhibits H5N1 replication. In order to understand the role of CEACAM1 in influenza pathogenesis, A549 and ATII cells were transfected with siCEACAM1 to knock-down endogenous CEACAM1 protein expression. ATII and A549 cells were transfected with siCEACAM1 or siNeg negative control. The expression of four main *CEACAM1* variants, *CEACAM1-4L*, *-4S*, *-3L* and *-3S*, and CEACAM1 protein were analyzed using SYBR Green qRT-PCR and Western blotting, respectively. SYBR Green qRT-PCR analysis showed that ATII cells transfected with 15 pmol of siCEACAM1 significantly reduced the expression of *CEACAM1-4L* and *-4S* when compared to siNeg control, while the expression of *CEACAM1-3L* and *-3S* was not altered (Fig. 4A). CEACAM1 protein expression was reduced by approximately 50% in both ATII and A549 cells following siCEACAM1 transfection when compared with siNeg-transfected cells (Fig. 4B). Increasing doses of siCEACAM1 (10, 15 and 20 pmol) did not further downregulate CEACAM1 protein expression in A549 cells (Fig. 4B). As such, 15 pmol of siCEACAM1 was chosen for subsequent knockdown studies in both ATII and A549 cells. It is important to note that the anti-CEACAM1 antibody only detects L isoforms based on epitope information provided by Abcam. Therefore, observed reductions in CEACAM1 protein expression can be attributed mainly to the abolishment of CEACAM1-4L.

The functional consequences of CEACAM1 knockdown were then examined in ATII and A549 cells following H5N1 infection. *IL6*, *IFNB1*, *CXCL10*, *CCL5* and *TNF* production was analyzed in H5N1-infected ATII and A549 cells using qRT-PCR. ATII (Fig. 5A) and A549 cells (Fig. 5B) transfected with siCEACAM1 showed significantly lower expression of *IL6*, *CXCL10* and *CCL5* when compared with siNeg-transfected cells. However, the expression of the anti-viral cytokine, *IFNB1*, was not affected in both cells types. In addition, *TNF* expression, which can be induced by type I IFNs[33], was significantly lower in siCEACAM1-transfected A549 cells (Fig. 5B), but was not affected in siCEACAM1-transfected ATII cells (Fig. 5A). Hypercytokinemia or "cytokine storm" in H5N1 and H7N9 virus-infected patients is thought to contribute to inflammatory tissue damage[34,35]. Downregulation of CEACAM1 in the context of severe viral infection may reduce inflammation caused by H5N1 infection without dampening the antiviral response. Furthermore, virus replication was significantly reduced by 5.2-fold in ATII (Figs. 5C) and 4.8-fold in A549 cells (Fig. 5D) transfected with siCEACAM1 when compared with siNeg-transfected cells. Virus titers in siNeg-transfected control cells were not significantly different from those observed in mock-transfected control cells (Fig. 5C,D).

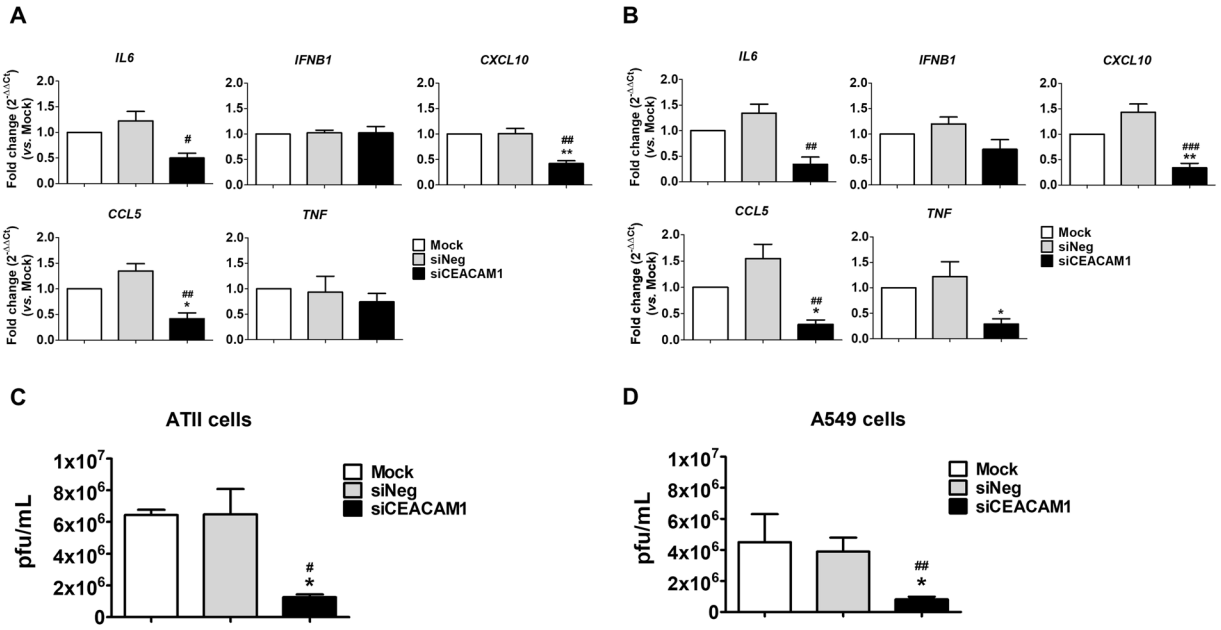

Figure 5. Knockdown of CEACAM1 inhibits H5N1 replication and H5N1-induced inflammation. ATII cells (**A**) and A549 cells (**B**) transfected with 15 pmol siCEACAM1 showed reduced cytokine and chemokine production in response to H5N1 infection as analyzed by qRT-PCR and compared to siNeg-transfected control cells. Plaque assay of H5N1 virus titers in ATII (**C**) and A549 (**D**) cells that were either mock-transfected or transfected with siCEACAM1 or siNeg. $^{*}p < 0.05$ and $^{**}p < 0.01$, compared with mock-transfected cells, $^{\#}p < 0.05$ and $^{\#\#}p < 0.01$, $^{\#\#}p < 0.001$, compared with siNeg-transfected cells. Experiments were performed using ATII cells from three donors and three different passages of A549 cells.

Discussion

Influenza viruses utilize host cellular machinery to manipulate normal cell processes in order to promote replication and evade host immune responses. Studies in the field are increasingly focused on understanding and modifying key host factors in order to ameliorate disease. Examples include modulation of ROS to reduce inflammation[5] and inhibition of NFκB and mitogenic Raf/MEK/ERK kinase cascade activation to suppress viral replication[36,37]. These host targeting strategies will offer an alternative to current interventions that are focused on targeting the virus. In the present study, we analyzed human host gene expression profiles following HPAI H5N1 infection and treatment with the antioxidant, apocynin. As expected, genes that were significantly upregulated following H5N1 infection were involved in biological processes, including cytokine signaling, immunity and apoptosis. In addition, H5N1-upregulated genes were also involved in regulation of protein phosphorylation, cellular metabolism and cell proliferation, which are thought to be exploited by viruses for replication[38]. Apocynin treatment had both anti-viral (Tables S2–S4)[5] and pro-viral impact (Fig. 2G), which is not surprising as ROS are potent microbicidal agents, as well as important immune signaling molecules at different concentrations[39]. In our hands, apocynin treatment reduced H5N1-induced inflammation, but also impacted the cellular defense response, cytokine production and cytokine-mediated signaling. Importantly, critical antiviral responses were not compromised, i.e. expression of pattern recognition receptors (e.g. *DDX58* (RIG-I), *TLR*s, *IFIH1* (MDA5)) was not downregulated (Table S1). Given the significant interference of influenza viruses on host immunity, we focused our attention on key regulators of the immune response. Through HiSeq analysis, we identified the cell adhesion molecule CEACAM1 as a critical regulator of immunity. Knockdown of endogenous CEACAM1 inhibited H5N1 virus replication and reduced H5N1-stimulated inflammatory cytokine/chemokine production.

H5N1 infection resulted in significant upregulation of a number of inflammatory cytokines/chemokines genes, including AXL and STING, which were significantly reduced by apocynin treatment to a level lower than that observed in uninfected cells (Table S4). It has been previously demonstrated that anti-AXL antibody treatment of PR8-infected mice significantly reduced lung inflammation and virus titers[40]. STING has been shown to be important for promoting anti-viral responses, as STING-knockout THP-1 cells produce less type I IFN following influenza A virus infection[41]. Reduction of STING gene expression or other anti-viral factors (e.g. IFNB1, MX1, ISG15; Table S1) by apocynin, may in part, explain the slight increase in influenza gene transcription following apocynin treatment (Fig. 2G). These results also suggest that apocynin treatment may reduce H5N1-induced inflammation and apoptosis. Indeed, the anti-inflammatory and anti-apoptotic effects of apocynin have been shown previously in a number of disease models, including diabetes mellitus[42], myocardial infarction[43], neuroinflammation[44] and influenza virus infection[6].

Recognition of intracellular viral RNA by pattern recognition receptors (PRRs) triggers the release of pro-inflammatory cytokines/chemokines that recruit innate immune cells, such as neutrophils and NK cells, to the site of infection to assist in viral clearance[45]. Neutrophils exert their cytotoxic function by first attaching to influenza-infected epithelial cells via adhesion molecules, such as CEACAM1[46]. Moreover, studies have indicated

that influenza virus infection promotes neutrophil apoptosis[47], delaying virus elimination[48]. Phosphorylation of CEACAM1 ITIM motifs and activation of caspase-3 is critical for mediating anti-apoptotic events and for promoting survival of neutrophils[27]. This suggests that CEACAM1-mediated anti-apoptotic events may be important for the resolution of influenza virus infection *in vivo*, which can be further investigated through infection studies with *Ceacam1*-knockout mice.

NK cells play a critical role in innate defense against influenza viruses by recognizing and killing infected cells. Influenza viruses, however, employ several strategies to escape NK effector functions, including modification of influenza hemagglutinin (HA) glycosylation to avoid NK activating receptor binding[49]. Homo- or heterophilic CEACAM1 interactions have been shown to inhibit NK-killing[25,26], and are thought to contribute to tumor cell immune evasion[50]. Given these findings, one could suggest the possibility that upregulation of CEACAM1 (to inhibit NK activity) may be a novel and uncharacterized immune evasion strategy employed by influenza viruses. Our laboratory is now investigating the role of CEACAM1 in NK cell function. Small-molecule inhibitors of protein kinases or protein phosphatases (e.g. inhibitors for Src, JAK, SHP2) have been developed as therapies for cancer, inflammation, immune and metabolic diseases[51]. Modulation of CEACAM1 phosphorylation, dimerization and the downstream function with small-molecule inhibitors may assist in dissecting the contribution of CEACAM1 to NK cell activity.

The molecular mechanism of CEACAM1 action following infection has also been explored in A549 cells using PR8 virus[52]. Vitenshtein *et al.* demonstrated that CEACAM1 was upregulated following recognition of viral RNA by RIG-I, and that this upregulation was interferon regulatory factor 3 (IRF3)-dependent. In addition, phosphorylation of CEACAM1 by SHP2 inhibited viral replication by reducing phosphorylation of mammalian target of rapamycin (mTOR) to suppress global cellular protein production. In the present study, we used a more physiologically relevant infection model, primary human ATII cells, to study the role of CEACAM1 in influenza virus infection, focusing on HPAI H5N1 virus. Consistent with findings from Vitenshtein *et al.*, significant upregulation of CEACAM1 protein was observed following influenza virus infection, especially in HPAI H5N1-infected cells. However, in contrast to the inhibitory effects of CEACAM1 on influenza virus replication observed by Vitenshtein *et al.*, knockdown of endogenous CEACAM1 protein expression reduced HPAI H5N1 titers by 4.8-fold in ATII cells. Despite the use of two different *in vitro* experimental settings, different influenza virus strains, infection doses and time points, both studies agree that CEACAM1 plays an important role in influenza virus infection and warrants further investigation.

Further studies will be required to investigate/confirm the molecular mechanisms of CEACAM1 upregulation following influenza virus infection, especially *in vivo*. As upregulation of CEACAM1 has been observed in other virus infections, such as cytomegalovirus[18] and papillomavirus[19], it will be important to determine whether a common mechanism of action can be attributed to CEACAM1 in order to determine its functional significance. If this can be established, CEACAM1 could be used as a target for the development of a pan-antiviral agent.

In summary, molecules on the cell surface such as CEACAM1 are particularly attractive candidates for therapeutic development, as drugs do not need to cross the cell membrane in order to be effective. Targeting of host-encoded genes in combination with current antivirals and vaccines may be a way of reducing morbidity and mortality associated with influenza virus infection. Our study clearly demonstrates that increased CEACAM1 expression is observed in primary human ATII cells infected with HPAI H5N1 influenza virus. Importantly, knockdown of CEACAM1 expression resulted in a reduction in influenza virus replication and suggests targeting of this molecule may assist in improving disease outcomes.

Materials and Methods

Isolation and culture of primary human ATII cells. Human non-tumor lung tissue samples were donated by anonymous patients undergoing lung resection at University Hospital, Geelong, Australia. The research protocols and human ethics were approved by the Human Ethics Committees of Deakin University, Barwon Health and the Commonwealth Scientific and Industrial Research Organisation (CSIRO). Informed consent was obtained from all tissue donors. All research was performed in accordance with the guidelines stated in the *National Statement on Ethical Conduct in Human Research (2007)*. The sampling of normal lung tissue was confirmed by the Victorian Cancer Biobank, Australia. Lung specimens were preserved in Hartmann's solution (Baxter) for 4–8 hours or O/N at 4 °C to maintain cellular integrity and viability before cells are isolated. Human alveolar epithelial type II (ATII) cells were isolated and cultured using a previously described method[30,53] with minor modifications. Briefly, lung tissue with visible bronchi was removed and perfused with abundant PBS and submerged in 0.5% Trypsin-EDTA (Gibco) twice for 15 min at 37 °C. The partially digested tissue was sliced into sections and further digested in Hank's Balanced Salt Solution (HBSS) containing elastase (12.9 units/mL; Roche Diagnostics) and DNase I (0.5 mg/mL; Roche Diagnostics) for 60 min at 37 °C. Single cell suspensions were obtained by filtration through a 40 μm cell strainer and cells (including macrophages and fibroblasts) were allowed to attach to tissue-culture treated Petri dishes in a 1:1 mixture of DMEM/F12 medium (Gibco) and small airway growth medium (SAGM) medium (Lonza) containing 5% fetal calf serum (FCS) and 0.5 mg/mL DNase I for 2 hours at 37 °C. Non-adherent cells, including ATII cells, were collected and subjected to centrifugation at 300 g for 20 min on a discontinuous Percoll density gradient (1.089 and 1.040 g/mL). Purified ATII cells from the interface of two density gradients was collected, washed in HBSS, and re-suspended in SAGM medium supplemented with 1% charcoal-filtered FCS (Gibco) and 100 units/mL penicillin and 100 μg/mL streptomycin (Gibco). ATII cells were plated on polyester Transwell inserts (0.4 μm pore; Corning) coated with type IV human placenta collagen (0.05 mg/mL; Sigma) at 300,000 cells/cm^2 and cultured under liquid-covered conditions in a humidified incubator (5% CO_2, 37 °C). Growth medium was changed every 48 hours. These culture conditions suppressed fibroblasts expansion within the freshly isolated ATII cells and encouraged ATII cells to form confluent monolayers with a typical large and somewhat square morphology[54] with increased expression of surfactant protein C (SPC) (data not shown).

Cell culture and media. A549 carcinomic human alveolar basal epithelial type II-like cells and Madin-Darby canine kidney (MDCK) cells were provided by the tissue culture facility of Australian Animal Health Laboratory (AAHL), CSIRO. A549 and MDCK cells were maintained in Ham's F12K medium (GIBCO) and RPMI-1640 medium (Invitrogen), respectively, supplemented with 10% FCS, 100 U/mL penicillin and 100 µg/mL streptomycin (GIBCO) and maintained at 37 °C, 5% CO_2.

Virus and viral infection. HPAI A/chicken/Vietnam/0008/2004 H5N1 (H5N1) was obtained from AAHL, CSIRO. Viral stocks of A/Puerto Rico/8/1934 H1N1 (PR8) were obtained from the University of Melbourne. Virus stocks were prepared using standard inoculation of 10-day-old embryonated eggs. A single stock of virus was prepared for use in all assays. All H5N1 experiments were performed within biosafety level 3 laboratories (BSL3) at AAHL, CSIRO.

Cells were infected with influenza A viruses as previously described[6,29]. Briefly, culture media was removed and cells were washed with warm PBS three times followed by inoculation with virus for 1 hour. Virus was then removed and cells were washed with warm PBS three times, and incubated in the appropriate fresh serum-free culture media containing 0.3% BSA at 37 °C. Uninfected and infected cells were processed identically. For HiSeq analysis, ATII cells from three donors were infected on the apical side with H5N1 at a MOI of 2 for 24 hours in serum-free SAGM medium supplemented with 0.3% bovine serum albumin (BSA) containing 1 mM apocynin dissolved in DMSO or 1% DMSO vehicle control. Uninfected ATII cells incubated in media containing 1% DMSO were used as a negative control. For other subsequent virus infection studies, ATII cells from a different set of three donors (different from those used in HiSeq analysis) or A549 cells from at least three different passages were infected with influenza A viruses at various MOIs as indicated in the text. For H5N1 studies following transfection with siRNA, the infectious dose was optimized to a MOI of 0.01, a dose at which significantly higher CEACAM1 protein expression was induced with minimal cell death at 24 hpi. For PR8 infection studies, a final concentration of 0.5 µg/mL L-1-Tosylamide-2-phenylethyl chloromethyl ketone (TPCK)-treated trypsin (Worthington) was included in media post-inoculation to assist replication. Virus titers were determined using standard plaque assays in MDCK cells as previously described[55].

RNA extraction, quality control (QC) and HiSeq analysis. ATII cells from three donors were used for HiSeq analysis. Total RNA was extracted from cells using a RNeasy Mini kit (Qiagen). Influenza-infected cells were washed with PBS three times and cells lysed with RLT buffer supplemented with β-mercaptoethanol (10 µL/mL; Gibco). Cell lysates were homogenized with QIAshredder columns followed by on-column DNA digestion with the RNase-Free DNase Set (Qiagen), and RNA extracted according to manufacturer's instructions. Initial QC was conducted to ensure that the quantity and quality of RNA samples for HiSeq analysis met the following criteria; 1) RNA samples had OD260/280 ratios between 1.8 and 2.0 as measured with NanoDrop™ Spectrophotometer (Thermo Scientific); 2) Sample concentrations were at a minimum of 100 ng/µl; 3) RNA was analyzed by agarose gel electrophoresis. RNA integrity and quality were validated by the presence of sharp clear bands of 28S and 18S ribosomal RNA, with a 28S:18S ratio of 2:1, along with the absence of genomic DNA and degraded RNA. As part of the initial QC and as an indication of consistent H5N1 infection, parallel quantitative real-time reverse transcriptase PCR (qRT-PCR) using the same RNA samples used for HiSeq analysis was performed in duplicate as previously described[6] to measure mRNA expression of *IL6*, *IFNB1*, *CXCL10*, *CCL5*, *TNF*, *SOCS1* and *SOCS3*, all of which are known to be upregulated following HPAI H5N1 infection of A549 cells[6]. RNA samples were stored in 0.1 volumes of 3 M Sodium Acetate (pH7.5 in DEPC-treated water) and 2 volumes of 100% Ethanol and submitted to Macrogen Inc. (Seoul, Republic of Korea) for HiSeq analysis (Illumina HiSeq 2000 Sequencing System, 100 bp paired-end sequencing).

Sequencing analysis and annotation. After confirming checksums and assessing raw data quality of the FASTQ files with FASTQC, RNA-Seq reads were processed according to standard Tuxedo pipeline protocols[56], using the annotated human genome (GRCh37, downloaded from Illumina iGenomes) as a reference. Briefly, raw reads for each sample were mapped to the human genome using TopHat2, sorted and converted to SAM format using Samtools and then assembled into transcriptomes using Cufflinks. Cuffmerge was used to combine transcript annotations from individual samples into a single reference transcriptome, and Cuffquant was used to obtain per-sample read counts. Cuffdiff was then used to conduct differential expression analysis. All programs were run using recommended parameters. It is important to note that the reference gtf file provided to cuffmerge was first edited using a custom python script to exclude lines containing features other than exon/cds, and contigs other than chromosomes 1–22, X, Y.

GO term and KEGG enrichment. Official gene IDs for transcripts that were differentially modulated following HPAI H5N1 infection with or without apocynin treatment were compiled into six target lists from pairwise comparisons ("ND *vs.* HD Up", "ND *vs.* HD Down", "ND *vs.* HA Up", "ND *vs.* HA Down", "HD *vs.* HA Up", "HD *vs.* HA Down"). Statistically significant differentially expressed transcripts were defined as having $\geq$2-fold change with a Benjamini-Hochberg adjusted P value < 0.01. A background list of genes was compiled by retrieving all gene IDs identified from the present HiSeq analysis with FPKM > 1. Biological process GO enrichment was performed using Gorilla, comparing unranked background and target lists[57]. Redundant GO terms were removed using REVIGO[58]. Target lists were also subjected to KEGG pathway analysis using a basic KEGG pathway mapper[59] and DAVID Bioinformatics Resources Functional Annotation Tool[60,61].

Quantitative real-time reverse transcriptase polymerase chain reaction (qRT-PCR). mRNA concentrations of genes of interest were assessed and analyzed using qRT-PCR performed in duplicate as previously described[6]. Briefly, after total RNA extraction from influenza-infected cells, cDNA was

prepared using SuperScript™ III First-Strand Synthesis SuperMix (Invitrogen). Gene expression of various cytokines was assessed using TaqMan Gene Expression Assays (Applied Biosystems) with commercial TaqMan primers and probes, with the exception of the influenza Matrix (M) gene (forward primer 5′-CTTCTAACCGAGGTCGAAACGTA-3′; reverse primer 5′-GGTGACAGGATTGGTCTTGTCTTTA-3′; probe 5′-FAM-TCAGGCCCCCTCAAAGCCGAG-NFQ-3′)[62]. Specific primers[63] (Table S5) were designed to estimate the expression of *CEACAM1-4L*, *-4S*, *-3L and -3S* in ATII and A549 cells using iTaq Universal SYBR Green Supermix (Bio-Rad) according to manufacturer's instruction. The absence of nonspecific amplification was confirmed by agarose gel electrophoresis of qRT-PCR products (15 μL) (data not shown). Gene expression was normalized to *β-actin* mRNA using the $2^{-\Delta\Delta CT}$ method where expression levels were determined relative to uninfected cell controls. All assays were performed in duplicate using an Applied Biosystems® StepOnePlus™ Real-Time PCR System.

Western blot analysis. Protein expression of CEACAM1 was determined using Western blot analysis as previously described[6]. Protein concentrations in cell lysates were determined using EZQ® Protein Quantitation Kit (Molecular Probes™, Invitrogen). Equal amounts of protein were loaded on NuPAGE 4–12% Bis-Tris gels (Invitrogen), resolved by SDS/PAGE and transferred to PVDF membranes (Bio-Rad). Membranes were probed with rabbit anti-human CEACAM1 monoclonal antibody EPR4049 (ab108397, Abcam) followed by goat anti-rabbit HRP-conjugated secondary antibody (Invitrogen). Proteins were visualized by incubating membranes with Pierce enhanced chemiluminescence (ECL) Plus Western Blotting Substrate (Thermo Scientific) followed by detection on a Bio-Rad ChemiDoc™ MP Imaging System or on Amersham™ Hyperfilm™ ECL (GE Healthcare). To use β-actin as a loading control, the same membrane was stripped in stripping buffer (1.5% (w/v) glycine, 0.1% (w/v) SDS, 1% (v/v) Tween-20, pH 2.2) and re-probed with a HRP-conjugated rabbit anti-β-actin monoclonal antibody (Cell Signaling). In some cases, two SDS/PAGE were performed simultaneously with equal amounts of protein loaded onto each gel for analysis of CEACAM1 and β-actin protein expression in each sample, respectively. Protein band density was quantified using Fiji software (version 1.49J10)[64]. CEACAM1 protein band density was normalized against that of β-actin and expressed as fold changes compared to controls.

Knockdown of endogenous CEACAM1. ATII and A549 cells were grown to 80% confluency in 6-well plates then transfected with small interfering RNA (siRNA) targeting the human *CEACAM1* gene (siCEACAM1; s1976, Silencer® Select Pre-designed siRNA, Ambion®) or siRNA control (siNeg; Silencer® Select Negative Control No. 1 siRNA, Ambion®) using Lipofetamine 3000 (ThermoFisher Scientific) according to manufacturer's instructions. Transfection and silencing efficiency were evaluated after 48 hours by Western blot analysis of CEACAM1 protein expression and by qRT-PCR analysis of *CEACAM1* variants. In parallel experiments, virus replication and cytokine/chemokine production was analyzed in siCEACAM1- or siNeg-transfected cells infected with H5N1 virus (MOI = 0.01) at 24 hpi.

Statistical analysis. Differences between two experimental groups were evaluated using a Student's unpaired, two-tailed *t* test. Fold-change differences of mRNA expression (qRT-PCR) between three experimental groups was evaluated using one-way analysis of variance (ANOVA) followed by a Bonferroni multiple-comparison test. Differences were considered significant with a p value of <0.05. The data are shown as means ± standard error of the mean (SEM) from three or four individual experiments. Statistical analyses were performed using GraphPad Prism for Windows (v5.02).

Data Availability

All data generated or analyzed during this study are included in this published article or the supplementary information file. The raw and processed HiSeq data has been deposited to GEO (GSE119767; https://www.ncbi.nlm.nih.gov/geo/).

References

1. Herfst, S. *et al*. Airborne transmission of influenza A/H5N1 virus between ferrets. *Science* **336**, 1534–1541 (2012).
2. Imai, M. *et al*. Experimental adaptation of an influenza H5 HA confers respiratory droplet transmission to a reassortant H5 HA/H1N1 virus in ferrets. *Nature* **486**, 420–428 (2012).
3. Itoh, Y. *et al*. Emergence of H7N9 Influenza A Virus Resistant to Neuraminidase Inhibitors in Nonhuman Primates. *Antimicrob. Agents Chemother.* **59**, 4962–4973 (2015).
4. Chen, Y. *et al*. Human infections with the emerging avian influenza A H7N9 virus from wet market poultry: clinical analysis and characterisation of viral genome. *Lancet* **381**, 1916–1925 (2013).
5. Vlahos, R. *et al*. Inhibition of Nox2 oxidase activity ameliorates influenza A virus-induced lung inflammation. *PLoS Pathog.* **7**, e1001271 (2011).
6. Ye, S., Lowther, S. & Stambas, J. Inhibition of reactive oxygen species production ameliorates inflammation induced by influenza A viruses via upregulation of SOCS1 and SOCS3. *J. Virol.* **89**, 2672–2683 (2015).
7. Yatmaz, S. *et al*. Glutathione peroxidase-1 reduces influenza A virus-induced lung inflammation. *Am. J. Respir. Cell Mol. Biol.* **48**, 17–26 (2013).
8. Cameron, C. M. *et al*. Gene expression analysis of host innate immune responses during Lethal H5N1 infection in ferrets. *J. Virol.* **82**, 11308–11317 (2008).
9. Muramoto, Y. *et al*. Disease severity is associated with differential gene expression at the early and late phases of infection in nonhuman primates infected with different H5N1 highly pathogenic avian influenza viruses. *J. Virol.* **88**, 8981–8997 (2014).
10. Wang, J. *et al*. Innate immune response to influenza A virus in differentiated human alveolar type II cells. *Am. J. Respir. Cell Mol. Biol.* **45**, 582–591 (2011).
11. Prall, F. *et al*. CD66a (BGP), an adhesion molecule of the carcinoembryonic antigen family, is expressed in epithelium, endothelium, and myeloid cells in a wide range of normal human tissues. *J. Histochem. Cytochem.* **44**, 35–41 (1996).
12. Coutelier, J. P. *et al*. B lymphocyte and macrophage expression of carcinoembryonic antigen-related adhesion molecules that serve as receptors for murine coronavirus. *Eur. J. Immunol.* **24**, 1383–1390 (1994).

13. Kammerer, R., Hahn, S., Singer, B. B., Luo, J. S. & von Kleist, S. Biliary glycoprotein (CD66a), a cell adhesion molecule of the immunoglobulin superfamily, on human lymphocytes: structure, expression and involvement in T cell activation. *Eur. J. Immunol.* **28**, 3664–3674 (1998).
14. Thirion, G., Feliu, A. A. & Coutelier, J. P. CD66a (CEACAM1) expression by mouse natural killer cells. *Immunology* **125**, 535–540 (2008).
15. Berger, C. N., Billker, O., Meyer, T. F., Servin, A. L. & Kansau, I. Differential recognition of members of the carcinoembryonic antigen family by Afa/Dr adhesins of diffusely adhering *Escherichia coli* (Afa/Dr DAEC). *Mol. Microbiol.* **52**, 963–983 (2004).
16. Klaile, E. *et al*. Binding of Candida albicans to Human CEACAM1 and CEACAM6 Modulates the Inflammatory Response of Intestinal Epithelial Cells. *MBio* **8** (2017).
17. Virji, M. *et al*. Carcinoembryonic antigens are targeted by diverse strains of typable and non-typable Haemophilus influenzae. *Mol. Microbiol.* **36**, 784–795 (2000).
18. Markel, G. *et al*. Pivotal role of CEACAM1 protein in the inhibition of activated decidual lymphocyte functions. *J. Clin. Invest.* **110**, 943–953 (2002).
19. Albarran-Somoza, B. *et al*. CEACAM1 in cervical cancer and precursor lesions: association with human papillomavirus infection. *J. Histochem. Cytochem.* **54**, 1393–1399 (2006).
20. Gray-Owen, S. D. & Blumberg, R. S. CEACAM1: contact-dependent control of immunity. *Nat. Rev. Immunol.* **6**, 433–446 (2006).
21. Singer, B. B. *et al*. Carcinoembryonic antigen-related cell adhesion molecule 1 expression and signaling in human, mouse, and rat leukocytes: evidence for replacement of the short cytoplasmic domain isoform by glycosylphosphatidylinositol-linked proteins in human leukocytes. *J. Immunol.* **168**, 5139–5146 (2002).
22. Watt, S. M. *et al*. Homophilic adhesion of human CEACAM1 involves N-terminal domain interactions: structural analysis of the binding site. *Blood* **98**, 1469–1479 (2001).
23. Markel, G. *et al*. The critical role of residues 43R and 44Q of carcinoembryonic antigen cell adhesion molecules-1 in the protection from killing by human NK cells. *J. Immunol.* **173**, 3732–3739 (2004).
24. Huber, M. *et al*. The carboxyl-terminal region of biliary glycoprotein controls its tyrosine phosphorylation and association with protein-tyrosine phosphatases SHP-1 and SHP-2 in epithelial cells. *J. Biol. Chem.* **274**, 335–344 (1999).
25. Markel, G. *et al*. CD66a interactions between human melanoma and NK cells: a novel class I MHC-independent inhibitory mechanism of cytotoxicity. *J. Immunol.* **168**, 2803–2810 (2002).
26. Stern, N. *et al*. Carcinoembryonic antigen (CEA) inhibits NK killing via interaction with CEA-related cell adhesion molecule 1. *J. Immunol.* **174**, 6692–6701 (2005).
27. Singer, B. B. *et al*. CEACAM1 (CD66a) mediates delay of spontaneous and Fas ligand-induced apoptosis in granulocytes. *Eur. J. Immunol.* **35**, 1949–1959 (2005).
28. Ortenberg, R. *et al*. Novel immunotherapy for malignant melanoma with a monoclonal antibody that blocks CEACAM1 homophilic interactions. *Mol. Cancer Ther.* **11**, 1300–1310 (2012).
29. Lam, W. Y., Yeung, A. C., Chu, I. M. & Chan, P. K. Profiles of cytokine and chemokine gene expression in human pulmonary epithelial cells induced by human and avian influenza viruses. *Virol J.* **7**, 344 (2010).
30. Witherden, I. R. & Tetley, T. D. Isolation and Culture of Human Alveolar Type II Pneumocytes. *Methods Mol. Med.* **56**, 137–146 (2001).
31. Oostwoud, L. C. *et al*. Apocynin and ebselen reduce influenza A virus-induced lung inflammation in cigarette smoke-exposed mice. *Sci. Rep.* **6**, 20983 (2016).
32. Klaile, E. *et al*. Carcinoembryonic antigen (CEA)-related cell adhesion molecules are co-expressed in the human lung and their expression can be modulated in bronchial epithelial cells by non-typable Haemophilus influenzae, Moraxella catarrhalis, TLR3, and type I and II interferons. *Respir. Res.* **14**, 85 (2013).
33. Yarilina, A., Park-Min, K. H., Antoniv, T., Hu, X. & Ivashkiv, L. B. TNF activates an IRF1-dependent autocrine loop leading to sustained expression of chemokines and STAT1-dependent type I interferon-response genes. *Nat. Immunol.* **9**, 378–387 (2008).
34. de Jong, M. D. *et al*. Fatal outcome of human influenza A (H5N1) is associated with high viral load and hypercytokinemia. *Nat. Med.* **12**, 1203–1207 (2006).
35. Zhou, J. *et al*. Biological features of novel avian influenza A (H7N9) virus. *Nature* **499**, 500–503 (2013).
36. Ludwig, S. Targeting cell signalling pathways to fight the flu: towards a paradigm change in anti-influenza therapy. *J. Antimicrob. Chemother.* **64**, 1–4 (2009).
37. Ludwig, S., Planz, O., Pleschka, S. & Wolff, T. Influenza-virus-induced signaling cascades: targets for antiviral therapy? *Trends Mol. Med.* **9**, 46–52 (2003).
38. Ehrhardt, C. *et al*. Interplay between influenza A virus and the innate immune signaling. *Microbes Infect* **12**, 81–87 (2010).
39. de Keizer, P. L., Burgering, B. M. & Dansen, T. B. Forkhead box o as a sensor, mediator, and regulator of redox signaling. *Antioxid Redox Signal* **14**, 1093–1106 (2011).
40. Shibata, T., Habiel, D. M., Coelho, A. L. & Hogaboam, C. M. Axl receptor blockade protects from invasive pulmonary aspergillosis in mice. *J. Immunol.* **193**, 3559–3565 (2014).
41. Holm, C. K. *et al*. Influenza A virus targets a cGAS-independent STING pathway that controls enveloped RNA viruses. *Nat Commun* **7**, 10680 (2016).
42. Li, M. *et al*. Effects of apocynin on oxidative stress and expression of apoptosis-related genes in testes of diabetic rats. *Mol Med Rep* **7**, 47–52 (2013).
43. Qin, F., Simeone, M. & Patel, R. Inhibition of NADPH oxidase reduces myocardial oxidative stress and apoptosis and improves cardiac function in heart failure after myocardial infarction. *Free Radic. Biol. Med.* **43**, 271–281 (2007).
44. Dang, D. K. *et al*. Apocynin prevents mitochondrial burdens, microglial activation, and pro-apoptosis induced by a toxic dose of methamphetamine in the striatum of mice via inhibition of p47phox activation by ERK. *J. Neuroinflammation* **13**, 12 (2016).
45. Iwasaki, A. & Pillai, P. S. Innate immunity to influenza virus infection. *Nat. Rev. Immunol.* **14**, 315–328 (2014).
46. Ratcliffe, D. R., Nolin, S. L. & Cramer, E. B. Neutrophil interaction with influenza-infected epithelial cells. *Blood* **72**, 142–149 (1988).
47. Colamussi, M. L., White, M. R., Crouch, E. & Hartshorn, K. L. Influenza A virus accelerates neutrophil apoptosis and markedly potentiates apoptotic effects of bacteria. *Blood* **93**, 2395–2403 (1999).
48. Hashimoto, Y., Moki, T., Takizawa, T., Shiratsuchi, A. & Nakanishi, Y. Evidence for phagocytosis of influenza virus-infected, apoptotic cells by neutrophils and macrophages in mice. *J. Immunol.* **178**, 2448–2457 (2007).
49. Owen, R. E. *et al*. Alterations in receptor binding properties of recent human influenza H3N2 viruses are associated with reduced natural killer cell lysis of infected cells. *J. Virol.* **81**, 11170–11178 (2007).
50. Chen, Z. *et al*. CEACAM1 dampens antitumor immunity by down-regulating NKG2D ligand expression on tumor cells. *J. Exp. Med.* **208**, 2633–2640 (2011).
51. Sawyer, T. K. *et al*. Protein phosphorylation and signal transduction modulation: chemistry perspectives for small-molecule drug discovery. *Med. Chem.* **1**, 293–319 (2005).
52. Vitenshtein, A. *et al*. CEACAM1-Mediated Inhibition of Virus Production. *Cell Rep* **15**, 2331–2339 (2016).
53. Chan, M. C. *et al*. Proinflammatory cytokine responses induced by influenza A (H5N1) viruses in primary human alveolar and bronchial epithelial cells. *Respir. Res.* **6**, 135 (2005).
54. Fuchs, S. *et al*. Differentiation of human alveolar epithelial cells in primary culture: morphological characterization and synthesis of caveolin-1 and surfactant protein-C. *Cell Tissue Res.* **311**, 31–45 (2003).

55. Izzard, L. *et al*. miRNA modulation of SOCS1 using an influenza A virus delivery system. *J. Gen. Virol.* **95**, 1880–1885 (2014).
56. Trapnell, C. *et al*. Differential gene and transcript expression analysis of RNA-seq experiments with TopHat and Cufflinks. *Nat. Protoc.* **7**, 562–578 (2012).
57. Eden, E., Navon, R., Steinfeld, I., Lipson, D. & Yakhini, Z. GOrilla: a tool for discovery and visualization of enriched GO terms in ranked gene lists. *BMC Bioinformatics* **10**, 48 (2009).
58. Supek, F., Bosnjak, M., Skunca, N. & Smuc, T. REVIGO summarizes and visualizes long lists of gene ontology terms. *PLoS One* **6**, e21800 (2011).
59. Kanehisa, M. & Goto, S. KEGG: kyoto encyclopedia of genes and genomes. *Nucleic Acids Res.* **28**, 27–30 (2000).
60. Huang da, W. *et al*. Extracting biological meaning from large gene lists with DAVID. *Curr Protoc Bioinformatics* **Chapter 13**, Unit13 11 (2009).
61. Huang da, W., Sherman, B. T. & Lempicki, R. A. Systematic and integrative analysis of large gene lists using DAVID bioinformatics resources. *Nat. Protoc.* **4**, 44–57 (2009).
62. Duchamp, M. B. *et al*. Pandemic A(H1N1)2009 influenza virus detection by real time RT-PCR: is viral quantification useful? *Clin. Microbiol. Infect.* **16**, 317–321 (2010).
63. Singer, B. B. *et al*. Deregulation of the CEACAM expression pattern causes undifferentiated cell growth in human lung adenocarcinoma cells. *PLoS One* **5**, e8747 (2010).
64. Schindelin, J. *et al*. Fiji: an open-source platform for biological-image analysis. *Nat Methods* **9**, 676–682 (2012).

Acknowledgements

This study was supported by funding from The Molecular and Medical Research Strategic Research Centre (MMR SRC), Deakin University and The Geelong Centre for Emerging Infectious Diseases (GCEID) (to S.Y.), and by an Alfred Deakin Postdoctoral Research Fellowship (to S.Y.). The authors wish to thank AAHL CSIRO and the University of Melbourne for providing viruses. We thank Katie-Lee Alexander from Barwon Health Tissue Bank, and Samantha Arandelovic from St John of God Pathology, Geelong, for the coordination of human lung tissue collection and sampling.

Author Contributions

Conceived and designed the experiments: S.Y. Tissue donor recruitment and lung tissue collection: C.H.Y. Performed the experiments: S.Y. Analyzed the data: S.Y., C.J.C. Wrote the manuscript: S.Y., C.J.C., J.S.

Additional Information

Supplementary information accompanies this paper at https://doi.org/10.1038/s41598-018-33605-6.

Competing Interests: The authors declare no competing interests.

Publisher's note: Springer Nature remains neutral with regard to jurisdictional claims in published maps and institutional affiliations.